Graphical Abstract (for review)

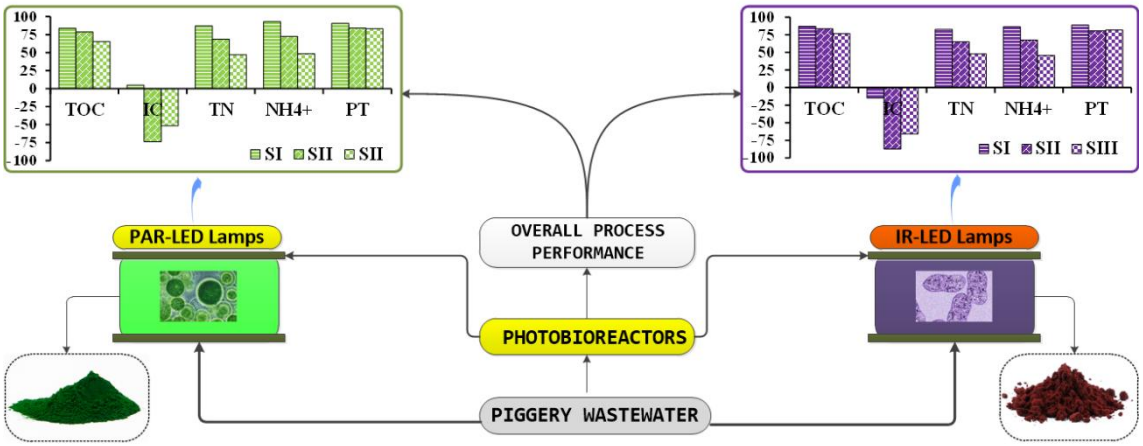

***Highlights (for review)**

- Photosynthetic bacteria and microalgae supported a similar piggery WW treatment
- Phototrophic bacteria exhibited higher organic carbon removal than microalgae
- HRT governed pollutant removal and biomass productivity in both photobioreactors
- Microalgae and bacteria population structure was determined by HRT

*Manuscript
Click here to view linked References

A systematic comparison of the potential of microalgae-bacteria and purple phototrophic bacteria consortia for the continuous treatment of piggery wastewater

Dimas García[1,2,3], Ignacio de Godos[1,2,5], Christian Domínguez[1], Sara Turiel[4], Silvia Bolado[1,2], Raúl Muñoz[1,2]*

[1]Department of Chemical Engineering and Environmental Technology, School of Industrial Engineering, Valladolid University, Dr. Mergelina, s/n, 47011, Valladolid, Spain

[2]Institute of Sustainable Processes, Dr. Mergelina, s/n, 47011, Valladolid, Spain

[3]Centro para la Investigación en Recursos Acuáticos de Nicaragua, CIRA/UNAN-Managua, Apdo. Postal 4598, Nicaragua

[4]The Institute of the Environment, La Serna 58 - 24007, León, Spain

[5]School of Forestry, Agronomic and Bioenergy Industry Engineering (EIFAB), Valladolid University, Campus Duques de Soria, Soria, Spain.

*corresponding author: mutora@iq.uva.es

ABSTRACT

This study evaluated the performance of two open-photobioreactors operated with microalgae-bacteria (PBR-AB) and purple photosynthetic bacteria (PBR-PPB) consortia during the continuous treatment of diluted (5%) piggery wastewater (PWW) at multiple hydraulic retention times (HRT). At a HRT of 10.6 days, PBR-AB supported the highest removal efficiencies of nitrogen, phosphorus and zinc (87±2, 91±3 and 98±1%), while the highest organic carbon removals were achieved in PBR-PPB (87±4%). The decrease in HRT from 10.6, to 7.6 and 4.1 day caused a gradual deterioration in organic material and nitrogen removal, but did not influence the removal of phosphorus and Zn. The decrease in HRT caused a severe wash-out of microalgae in PBR-AB and played a

key role in the structure of bacterial population in both photobioreactors. In addition, batch biodegradation tests at multiple PWW dilutions (5, 10 and 15%) confirmed the slightly better performance of algal-bacterial systems regardless of PWW dilution.

Keywords:
Algal-bacterial processes; photobioreactor; photosynthetic biodegradation; PPB; swine manure.

1. Introduction

The large volumes of wastewater yearly generated from domestic, industrial and agricultural activities demand a rapid and cost-effective wastewater treatment prior to discharge into natural water bodies. More specifically, an insufficient treatment of agroindustrial effluents, which rank among the highest strengths wastewaters, can cause severe episodes of eutrophication in surface water and pollution of groundwater (Mateo-sagasta and Burke, 2012). Only in the European Union, 215-430 Mm^3 of piggery wastewaters (PWW) with [COD] > 50 g/L or [TN] > 5 g/L are annually generated (García et al., 2018; statista, 2018). Conventional agricultural wastewater treatment (WWT) technologies (e.g. activated sludge, trickling filters) are highly energy intensive and entail a significant loss of valuable nutrients. In this context, photosynthetic treatments have emerged as a cost-effective alternative to conventional WWT based on their potential to support a superior nutrients and carbon recovery from agricultural wastewaters.

Photosynthetic WWT has been traditionally based on the cultivation of microalgae, which produce O_2 and assimilate nutrients using the visible spectrum of sunlight as

energy source, in symbiosis with heterotrophic and nitrifying bacteria. More specifically, microalgal-bacterial consortia can support efficient removals of organic matter, nutrients, heavy metals and pathogens as a result of their dual autotrophic and heterotrophic metabolism (Rittmann and McCarty, 2012). This symbiosis results in a low energy consumption and carbon footprint since the CO_2 generated during organic matter oxidation is photosynthetically fixed (Cheah et al., 2016; Dassey and Theegala, 2013). Algal-bacterial processes have been successfully tested for the treatment of domestic wastewater (García et al., 2017a; Oswald et al., 1957), centrates (Posadas et al., 2017), vinasse (Serejo et al., 2015), digested livestock effluents (Franchino et al., 2016; Tigini et al., 2016), parboiled rice wastewater (Bastos et al., 2009) and PWW (de Godos et al., 2010; García et al., 2018, 2017b).

On the other hand, purple phototrophic bacteria (PPB) can also use solar radiation (the infrared spectrum) as energy source during anoxygenic photosynthesis, which requires electron donors such as organic matter and nutrients to built-up PPB biomass (Bertling et al., 2006). PPB can support high rates of organic matter and nutrient assimilation and exhibit a high tolerance towards wastewater toxicity. Furthermore, there is an increasing interest in PPB-based WWT since PPB are able to synthesize polyhydroxybutyrates (PHB) and polyphosphates, and possess a more versatile metabolism than microalgae (Hülsen et al., 2014). PPB have been recently used to treat domestic wastewaters (Hülsen et al., 2016a, 2016b, 2014; Zhang et al., 2003), PWW (Myung et al., 2004), rubber sheet wastewater (Kantachote et al., 2005), pharmaceutical wastewater (Madukasi et al., 2010) and fish industry effluent (de Lima et al., 2011) with promising results. However, while microalgae-based WWT has been evaluated both indoors and outdoors in open and enclosed photobioreactors from lab scale to industrial facilities

(Craggs et al., 2012; de Godos et al., 2016), PPB-based WWT has been only evaluated indoors under lab scale conditions. In this context, there is a lack of comparative studies systematically assessing the treatment capacity of consortia of microalgae-bacteria and purple photosynthetic bacteria in order to elucidate the most suitable photosynthetic microbial group to support a cost-effective piggery wastewater treatment.

This work aimed at systematically evaluating the performance of open algal-bacterial and PPB photobioreactors for the indoor treatment of PWW under artificial illumination. The influence of the hydraulic retention time (HRT) on the removal of carbon, nitrogen, phosphorous and zinc (a heavy metal typically present in PWW that is used as growth promoting agent in swine nutrition), and on the structure of the algal-bacterial and PPB population was investigated. In addition, the influence of PWW dilution on the biodegradation performance of an algal-bacterial consortium and PPB was assessed batchwise.

2. Materials and methods

2.1. Inocula and piggery wastewater

A *Chlorella vulgaris* culture obtained from an outdoors high rate algal pond (HRAP) treating centrate was used as inoculum in the algal-bacterial photobioreactor. The PPB inoculum used was obtained from a batch enrichment in diluted PWW (17%) under continuous infrared (IR) light illumination at 50 W/m^2. Fresh PWW was collected from a nearby swine farm at Cantalejo (Spain) and stored at 4 °C. The PWW was centrifuged for 10 min at 10000 rpm before dilution to reduce the concentration of TSS. The average composition of the 5% diluted PWW is shown in Table 1. The inocula for the

batch biodegradation tests were taken from the photobioreactors under steady state conditions in Stage I.

2.2. *Batch PWW biodegradation tests*

An algal-bacterial (AB) batch test was conducted in three gas-tight glass bottles of 1.1 L illuminated by light-emitting diode (LED) lamps at 1380±24 μmol/m^2·s (302.2 W/m^2) for 12 hours a day (150 W PCB Clearflood 120 LED NW, Phillips, Spain). Similarly, a purple phototrophic bacteria (PPB) batch test was carried out in 1.1 L gas-tight glass bottles illuminated by IR lamps at 45±1 W/m^2 for 12 hours a day. Both light intensities were selected to simulate the natural sun radiation conditions of PAR and IR (García et al., 2017b; Hülsen et al., 2016a). The light intensities were measured at the liquid surface in the bottle. The bottles were initially filled with 400 mL of 5, 10 and 15% diluted PWW and inoculated with fresh biomass at 760 mg TSS/L. The algal-bacterial inoculum, obtained from the algal-bacterial photobioreactor (PBR-AB), was composed of *Chlamydomonas* sp., *Chlorella kessieri*, *Chlorella vulgaris* and *Scenedesmus acutus*, which represented 14, 23, 43 and 20% of the algal population, respectively. Similarly, the PPB inoculum, obtained from the PPB photobioreactor (PBR-PPB), was mainly composed of bacteria from the phyla *Proteobacteria*, *Synergistetes*, *Firmicutes*, which represented 83.8, 5.3 and 3.6 % of the bacterial population, respectively.

All bottles were flushed with N_2 for 10 minutes to establish an initial environment totally deprived from O_2. The tests were incubated at 30 ^oC (using thermostatic water baths) under continuous magnetic agitation (200 rpm). Liquid samples of 20 mL were periodically taken to determine the pH and concentration of total suspended solids (TSS), total organic carbon (TOC), inorganic carbon (IC) and total nitrogen (TN). In

addition, gas samples from the headspace of the bottles were daily drawn using gas-tight syringes to determine the gas concentration of N_2, CO_2 and O_2 by Gas Chromatography with Thermal Conductivity Detection. The injector and oven were set at 150°C, 18psi and a split ratio 3. The detector was operated at 200°C with a Helium makeup flow of 20 ml/min and a Helium ref/makeup flow of 30 ml/min.

2.3 *PWW biodegradation in continuous photobioreactors*

The experimental set-up consisted of two 3L open photobioreactors (0.15 m deep and 0.02 m^2 of superficial area). The PBR-AB was illuminated at 1393±32 µmol/m^2·s for 12 hours a day (04h00 to 16h00) using visible LED lamps arranged in a horizontal configuration 60 cm above the surface of the PBR (Fig. 1) (150 W PCB Clearflood 120 LED NW, Phillips, Spain). The PBR-PPB was illuminated at 48±4W/m^2 for 12 hours a day (04h00 to 16h00) by IR LED lamps arranged in a horizontal configuration 20 cm above the surface of the PBR (Fig. 1). The light intensities were measured in the surface of both photobioreactors. The PBR-AB was jacketed and connected to a cooling water bath to maintain similar temperatures in both PBRs. The cultivation broths of PBR-AB and PBR-PPB were mixed via two water immersion pumps. Both photobioreactors were initially filled with tap water (tap water was aerated prior to PWW dilution to degrade any residual chlorine), inoculated with fresh biomass at 275 mg TSS/L and fed with 5% diluted PWW using a 205U7CA multi-channel cassette pump (Watson-Marlow, UK) at HRTs of 10.6, 7.6 and 4.1 days in stage I, II and III, respectively (Table 1).

< Fig. 1>

Liquid samples from the influent PWW and the effluents of the photobioreactors were drawn weekly to determine the concentrations of TOC, IC, TN, NH_4^+, NO_3^-, NO_2^-, TP,

Zn and TSS. Likewise, the microalgae population structure in the photobioreactors was weekly assessed from biomass samples preserved with lugol acid at 5% and formaldehyde at 10%, and stored at 4 ºC prior to analysis. Cultivation broth samples from the photobioreactors were also collected under steady state conditions and immediately stored at -20 ºC to evaluate the richness and composition of the bacterial communities. Unfortunately, the analysis of absolute abundance of microorganisms was out of the scope of this study. Dissolved oxygen concentration (DO) and pH in the cultivation broth of the photobioreactors were daily measured, while the influents and effluents flow rates were daily recorded to monitor water evaporation losses. Finally, the C, N and P content of the biomass was monitored in both PBRs under steady state conditions.

The removal efficiencies (REs) of C (TOC-REs), N (TN-REs), P (TP-REs) and Zn (Zn-REs) were calculated according to Eq. (1):

$$RE(\%) = \frac{(C_{inf} \times Q_{inf}) - (C_{eff} \times Q_{eff})}{C_{inf} \times Q_{inf}} \times 100 \quad (1)$$

where C_{inf} and C_{eff} represent the concentrations of TOC, IC, TN, TP and Zn in the influent PWW and PBR effluents, respectively, while Q_{inf} and Q_{eff} represent the influents and effluents flow rates, respectively. The process was considered under steady state when the TSS concentrations in the photobioreactors remained constant for at least four consecutive samplings. The results here provided correspond to the average ± standard deviation from duplicate measurements drawn weekly along one month of steady state operation.

<Table 1>

2.4 Analytical procedures

A 510 pH meter (EUTECH Instrument, The Netherlands) was used to measure the pH, while a CellOX® 325 oximeter was used to measure the dissolved oxygen and temperature (WTW, Germany). Photosynthetic active radiation (PAR) was measured with a LI-250A light meter (LI-COR Biosciences, Germany), while the intensity of infrared radiation was determined with a PASPort light meter (PASCO airlink®, California. USA). TOC, IC and TN concentrations were determined using a TOC-V CSH analyzer equipped with a TNM-1 module (Shimadzu, Japan). NO_2^- and NO_3^- concentrations were analyzed by High Performance Liquid Chromatography - Ion Chromatography (HPLC-IC) with a Waters 515 HPLC pump coupled with a Waters 432 ionic conductivity detector and equipped with an IC-Pak Anion HC (150 mm × 4.6 mm) Waters column (García et al., 2017a). TP, $N\text{-}NH_4^+$ and TSS concentrations were determined according to Standard Methods (APHA, 2005). The analysis of the C, N and P content in pre-dried and grinded biomass was carried out using a LECO CHNS-932 elemental analyzer. Zinc was determined using a 725-ICP Optical Emission Spectrophotometer (Agilent, USA) at 213.62 nm.

Microalgae were identified and quantified by microscopic examination (OLYMPUS IX70, USA) according with phytoplankton manual (Sournia, 1978). Molecular analysis of the bacterial populations in PBR-AB and PBR-PPB was conducted according to García et al., (2017b). The genomic deoxyribonucleic acid (DNA) was extracted from inocula and photobioreactors effluents, respectively, by FastDNASpin Kit for Soil (MP Biomedicals, LLC, USA) according to the manufacturer's protocol. An aliquot of 300 ng DNA of each sample was provided to Fundació per al Foment de la Investigació Sanitária i Biomédica de la Comunitat Valenciana (FISABIO, Valencia, Spain) for 16S

rDNA analyses. Gene amplicons were amplified following the protocol for 16S rDNA gene Metagenomic Sequencing Library Preparation Illumina (Cod. 15044223 Rev. A). The gene-specific sequences used in this protocol targeted the 16S rDNA gene V3 and V4 region. Illumina adapter overhang nucleotide sequences were added to the gene-specific sequences. The primers were selected according to Klindworth et al. (2013). The sequence for the 16S rDNA gene Amplicon PCR Forward Primer was 5´TCGTCGGCAGCGTCAGATGTGTATAAGAGACAGCCTACGGGNGGCWGCAG; the sequence for the 16S rDNA gene Amplicon PCR Reverse Primer = 5' was GTCTCGTGGGCTCGGAGATGTGTATAAGAGACAGGACTACHVGGGTATCTAATCC.

An aliquot of 5 ng/µl of genomic DNA (in 10 mM Tris pH 8.5) was used to initiate the protocol. After 16S rDNA gene amplification, the mutiplexing step was performed using Nextera XT Index Kit (FC-131-1096). An aliquot of 1 µl of the PCR product on a Bioanalyzer DNA 1000 chip was used to verify the size (expected size on a Bioanalyzer trace was ~550 bp). After size verification, the libraries were sequenced using a 2×300pb paired-end run (MiSeq Reagent kit v3 (MS-102-3001)) on a MiSeq Sequencer according to manufacturer's instructions (Illumina). Data Quality assessment was performed by using the prinseq-lite program with the following parameters: min_length of 50 bp and trim_qual_right of 30. The reads for filtered samples ranged between 92128 and 122324, for denoised samples ranged between 92128 and 122324, for merged samples between 13805 and 45299, and for non-chimeric between 13683 and 44503.

Finally, the Shannon-Wiener diversity index (*H*) was determined using the peak heights in the densitometric curves. This index, which represents both the sample richness and

evenness and ranges from 1.5 to 3.5 (low and high species evenness and richness, respectively), was calculated according to Eq. (2) (MacDonald, 2003):

$$H = -\sum[P_i ln(P_i)] \quad (2)$$

where P_i is the importance probability of the bands in a lane ($P_i = n_i/n$), n_i is the height of an individual peak and n is the sum of all peak heights in the densitometric curves).

3. Results and Discussion

3.1. Batch PWW biodegradation tests

Overall, slightly higher TOC and TN removals were recorded in algal-bacterial tests during batch PWW treatment compared to the tests conducted with PPB. The final TOC-REs in AB tests carried out with 5, 10 and 15% diluted PWW (namely AB-5, AB-10 and AB-15, respectively) accounted for 62, 46, 64%, respectively, compared to 52, 45 and 50% in PPB tests at comparable dilutions (namely PPB-5, PPB-10 and PPB-15, respectively). AB and PPB tests experienced a rapid decrease in organic matter concentration during the first 165 hours, with no significant variation in TOC concentration until the end of the experiment (Fig. 2a). The higher organic carbon removal in AB tests can be attributed to differences in microbial population structure and the occurrence of aerobic conditions. Hence, the aerobic bacteria present in the AB consortium were likely capable of utilizing a wider spectrum of organic compounds as electron donors than PPB (Golomysova et al., 2010). The results herein obtained in AB tests were in agreement with the study conducted by de Godos et al., (2010), who recorded TOC-REs of 55, 42, 42 and 46% during the biodegradation of 8 fold diluted PWW with *E. viridis*, *S. obliquus*, *C. sorokiniana* and *Chlorella* sp, respectively, in symbiosis with activated sludge. However, Hülsen et al., (2018) reported lower total

and soluble COD-REs (< 20% and < 40%, respectively) during the batch treatment of PWW by PPB.

The final removals of TN accounted for 47, 48 and 66% in AB-5, AB-10 and AB-15, respectively, and 43, 43 and 55% in PPB-5, PPB-10 and PPB-15, respectively (Fig. 2b). An active removal of nitrogen was detected during the first 165 hours of assay in both test series, which suggested the assimilatory nature of the N removal mechanism (correlated to TOC removal). The results herein obtained in AB tests were similar to those reported by de Godos et al., (2010), who recorded TN-REs ranging from 25 to 46% during the batch biodegradation of 8 fold diluted PWW. However, Hülsen et al., (2018) reported TN and NH_4^+ REs < 10% and < 40%, respectively, during the batch treatment of PWW by PPB.

On the other hand, the final biomass concentrations in AB-5, AB-10 and AB-15 accounted for 750, 1520, 2000 mg TSS/L, respectively, and 820, 1290 and 1460 mg TSS/L in PPB-5, PPB-10 and PPB-15, respectively (Fig. 2c). In this context, the higher TOC-REs and TN-REs recorded in AB tests supported the higher biomass concentrations here observed compared to PPB tests (García et al., 2017a), although the reasons underlying the slightly higher TSS concentration in PPB-5 compared to AB-5 remained unclear.

< Fig. 2>

3.2. PWW biodegradation in continuous photobioreactors

3.2.1 Carbon, nitrogen and phosphorous removal

A gradual deterioration in the REs of carbon and nitrogen was recorded when decreasing the HRT in both PBRs. Indeed, TOC-REs in PBR-AB averaged 84±4, 79±3 and 66±3% in Stage I (SI), Stage II (SII) and Stage III (SIII), respectively, which resulted in steady state TOC concentrations in the effluent of 309±18, 199±9 and 246±31 mg/L, respectively (Fig.3a, Table 1). The results herein obtained confirmed the consistent removals of organic matter from PWW by algal-bacterial consortia and were in agreement with García et al., (2017b), who reported TOC-REs ranging from 85 to 94% in 3 L HRAPs during the treatment of 20 and 10 folds diluted PWW at a HRT of 27 days. Likewise, Hernández et al., (2013) reported COD-REs of 62±2 % in an outdoors 5 L HRAP treating PWW at 10 days of HRT. On the other hand, the TOC-REs in PBR-PPB accounted for 87±4, 84±3 and 77±5% in SI, SII and SIII, respectively, which entailed average TOC concentrations in the effluent lower than those detected in PBR-AB: 181±54, 136±3 and 156±31 mg/L, respectively (Fig.3a, Table 1). The TOC-REs here achieved were higher than the average organic matter removals recorded by González et al., (2017) (REs ~65%) during the treatment of an anaerobic effluent in a 32 L membrane photobioreactor operated with native PPB. The high TOC-REs herein recorded in PBR-PPB could be attributed to the higher metabolic versatility of PPB, which degraded organic matter both aerobically (mediated by O_2 diffusion from the open atmosphere) and anaerobically (Hunter et al., 2009). In this context, Golomysova et al., (2010) highlighted the key role of the acetate assimilatory pathway of PPB during WWT. At this point, it must be also stressed that volatile fatty acids typically represent the main fraction of the soluble COD in PWW (González-Fernández and García-Encina, 2009). Finally, the ratio between the TOC removed (mg C/d) and the biomass produced (mgTSS/d) accounted for 0.68 and 1.33 in PBR-AB and PBR-PPB, respectively, during SI. These ratios amounted 0.77 and 0.73 in PBR-AB, and 0.88 and 0.96 in PBR-PPB

during SII and SIII, respectively, which confirmed the higher specific biodegradation potential of PPB compared to AB.

On the other hand, average IC concentrations in the effluent of 167±17, 144±10 and 177±10 mg/L were recorded during SI, SII and SIII, respectively (Fig.3b, Table 1). Likewise, steady state IC concentrations in the effluent of 142±3, 137±7 and 122±15 mg/L were observed in SI, SII and SIII, respectively (Fig.3b, Table 1). These higher IC concentrations recorded in the effluent of both PBRs compared to the IC concentration in the piggery wastewater evidenced the accumulation of inorganic carbon mediated by the active microbial TOC oxidation. This finding was in agreement with previous observations in HRAPs treating PWW (García et al., 2017b). Overall, the higher IC-REs during the treatment of PWW in PBR-AB were likely mediated by the higher biomass concentrations and the oxygenic nature of the photosynthesis prevailing in PBR-AB (Table 1). A carbon mass balance showed that bioassimilation was the main mechanism responsible for carbon removal in PBR-AB and PBR-PPB during SII and SIII, with C recoveries in the form of biomass ranging between 58 and 72% of the total carbon removed. Carbon removal by stripping (prior mineralization of the organic carbon to CO_2) was the main mechanism accounting for carbon removal in PBR-PPB during SI, with a contribution of 62% of the total carbon removed.

< Fig. 3>

The TN-REs in PBR-AB under steady state averaged 87±2, 69±3 and 47±1% in SI, SII and SIII, respectively, which corresponded to average TN concentrations in the effluent of 68±5, 85±3, and 118±9 mg/L, respectively (Fig. 3c, Table 1). Similar results were found in PBR-PPB, where TN-REs accounted respectively for 83±2, 65±6 and 48±3%,

respectively, resulting in average TN concentrations in the effluent of 65±4, 84±6, and 110±10 mg/L in SI, SII and SIII, respectively (Fig. 3c, Table 1). Steady state NH_4^+-REs of 93±1, 72±2 and 49±3% in PBR-AB and of 86±1, 68±5 and 48±4% in PBR-PPB were recorded during SI, SII, and SIII, respectively (Fig. 3d, Table 1). The TN-REs here achieved in PBR-AB were similar to those reported by García et al., (2018), who recorded TN removals of 82-85% during the treatment of 20 fold diluted PWW in indoor algal-bacterial open photobioreactors at a HRT of ≈ 27 days. However, these TN-REs were higher than the removals of 37±8% obtained by de Godos et al., (2010) during PWW treatment in a 3.5L indoor enclosed photobioreactor operated at a HRT of 4.4 days. The nitrogen mass balance conducted under steady state revealed that stripping was the main N removal mechanism in both PBRs during the three stages, with assimilation into biomass in PBR-AB accounting only for 15, 21 and 24% of the TN removed, in SI, SII and SIII, respectively. Similarly, nitrogen assimilation in PBR-PPB accounted for only 9, 19 and 29% of the TN removed in SI, SII and SIII, respectively.

Finally, TP-REs of 91±3, 84±4 and 83±3% were recorded in PBR-AB in SI, SII and SIII, respectively, which resulted in average TP concentrations in the effluent of 1.6±0.6, 1.6±0.4, and 1.2±0.3 mg/L, respectively (Fig. 3e, Table 1). On the other hand, the TP-REs in PBR-PPB accounted for 89±3, 81±1 and 82±9% in SI, SII and SIII, respectively, which entailed effluent TP concentrations of 1.3±0.5, 1.7±0.3, and 1.2±0.5 mg/L, respectively (Fig. 3e, Table 1). Interestingly, high TP-REs were recorded in both PBRs regardless of the HRT and biomass concentration. The TP-REs obtained in PBR-AB were similar to those reported by García et al., (2018) during the treatment of 15% diluted PWW in indoor algal-bacterial open photobioreactors (REs ~ from 90-92%.

These values were also higher than the TP-REs of 58% reported by Myung et al., (2004) during the treatment of PWW by PPB. Phosphorus assimilation into biomass was likely the main P removal mechanism based on the moderate pH values (8.5-8-7) prevailing in both PBRs (pH = 8.5-8.7), which were not likely to support a significant phosphate precipitation (Table 1) (García et al., 2017a). Indeed, a phosphorus mass balance to PBR-AB revealed that 97, 89 and 51% of the total phosphorus removed was recovered as biomass during SI, SII and SIII, respectively. Similar P recoveries (60-81%) were estimated in PBR-PPB.

3.2.2 Zinc removal

Zn-REs of 98±1, 94±2 and 91±2% were attained in PBR-AB in SI, SII and SIII, respectively, which mediated very low concentrations of Zn in the effluent under steady state conditions (0.07 ± 0.03, 0.08±0.02 and 0.08 ± 0.02 mg/L, respectively) (Table 1). On the other hand, the Zn -REs in PBR-PPB accounted for 93±1, 90±2 and 92±2% in SI, SII and SIII, respectively, which resulted in Zn effluent concentrations of 0.15±0.02, 0.12±0.02 and 0.06±0.01 mg/L, respectively (Fig. 3e, Table 1). The moderate pH prevailing in both PBRs (8.5-8-7) suggest that biosorption was likely the main mechanism governing Zn removal, although Zn-REs were not correlated with biomass concentrations (Javanbakht et al., 2014; Kaplan et al., 1987). The Zn-REs herein achieved were higher than those reported by García et al. (2017b) during PWW treatment in 3 L indoors HRAPs operated at a HRT of ≈27 days (71- 83%).

3.2.3 Concentration, productivity and composition of biomass

Biomass concentration in PBR-AB increased during SI from ≈237 mg TSS/L up to steady state concentrations of 2640±161 mg TSS/L by days 63-84. A rapid decrease of

biomass concentration to 1005±54 mg TSS/L in SII and to 683±35 mg TSS/L in SIII occurred as a result of the stepwise decrease in HRT in PBR-AB (Fig. 4, Table 1). On the other hand, the biomass concentration in PBR-PPB experienced a gradual increase during the first 28 days of operation and stabilized at 873±114 mg TSS/L. Despite the decrease in HRT from 10.6 to 7.6 days did not result in a significant variation in TSS concentration in PBR-PPB (853±51 mg TSS/L in SII), a gradual decrease to 553±118 mg TSS/L occurred during SIII mediated by the decrease in HRT to 4.1 days (Fig.4). The higher biomass concentrations recorded in PBR-AB compared to PBR-PPB, which were more evident during SI, were likely due to the active photosynthetic CO_2 assimilation by microalgae. These differences in biomass concentrations between both PBRs could be also explained by the slightly higher evaporation rates recorded in PBR-AB induced by its slightly higher temperatures. Hence, water evaporation (estimated as the ratio between the flow rate of water evaporation and the influent flow rate) in SI, SII and SIII accounted for 72, 42 and 21% in PBR-AB, and 56, 36 and 18% in PBR-PPB, respectively. At this point it should be highlighted that the working volume of the PBRs remained constant at 3L despite the high evaporation rates recorded.

The lowest areal biomass productivities were recorded in SI in both PBRs, accounting for 10.4 and 5.4 $g/m^2 \cdot d$ in PBR-AB and PBR-PPB, respectively. The decrease in HRT resulted in increased biomass productivities up to 11.5 and 10.8 $g/m^2 \cdot d$ in stage II in PBR-AB and PBR-PPB, respectively. Finally, process operation at a HRT of 4.1 days was characterized by the highest biomass productivities: 18.4 $g/m^2 \cdot d$ in PBR-AB and 16.6 $g/m^2 \cdot d$ in PBR-PPB.

The C, N and P content of the algal-bacterial biomass averaged 48 ± 4, 7.5 ± 1.4 and 0.62 ± 0.15%, and 52 ± 1, 8.4 ± 0.5 and 0.69± 0.05% in the PPB biomass, with no clear correlation with the HRT. The algal-bacterial biomass composition was similar to the values reported by Cabanelas et al., (2013), who determined a C, N and P content in the harvested biomass of ≈ 44, 7.5 and 0.5%, respectively, in a photobioreactor inoculated with *C. vulgaris* and supplemented with CO_2 during the treatment of settled domestic wastewater.

< Fig. 4>

3.2.4 Microalgae population structure

C. vulgaris represented the dominant species in PBR-AB from day 1 to day 84 in SI, with a maximum concentration of $1.6 \cdot 10^{10}$ cells/L by day 35 (corresponding to 90 % of the total cell number) (Fig. 5a). Interestingly, a severe decrease in the total number of microalgae cells was observed from day 35 to day 56, which remained stable at $1.8 \pm 0.2 \cdot 10^{9}$cells/L by the end of SI. *Chlorella kessieri* was always detected from day 42 to day 84, while *Scenedesmus acutus* and *Tetradesmus obliquus* were detected for 10 and 7 weeks during SI, respectively. On the other hand, no microalgae was detected in PBR-PPB during SI (Fig. 5b). During SII, *C. vulgaris* and *C. kessieri* were present in PBR-AB throughout the experimental period from day 91 to day147. *C. vulgaris* achieved a maximum concentration of $0.24 \cdot 10^{9}$ cells/L by day 105 (corresponding to 55 % of the total cell number). However, the maximum cell concentration was recorded by day 119, where $0.51 \cdot 10^{9}$cells/L and eight microalgae species were detected. S*c. acutus* and *Tet. obliquus (acutudesmus)* were not detected from days 98 and 126 onwards, respectively. On the other hand, *C. vulgaris* and *Chlorococcum sp.* were detected 6 and 2 times during SII in PBR-PPB, respectively. However, the maximum microalgae cell

concentration in PBR-PPB was only $0.01 \cdot 10^9$ cells/L, which was recorded by day 147 as a result of the occurrence of four microalgae species. Finally, *C. vulgaris* and *C. kessieri* were always present in SIII from day 154 to day 224 in PBR-AB, while *Chlorella minutissima* was identified from day 175 onwards. However, the maximum cell concentration of microalgae in PBR-AB during SIII was only $0.27 \cdot 10^9$cells/L (day 217). Finally, six microalgae species were detected in PBR-PPB during SIII. *Aphanothece saxicola* was detected by day 161 and day 217, while *C. vulgaris*, *C. kessieri* and *C. minutissima* were detected during SIII up to days 154, 161 and 182, respectively. The N_2 fixing cyanobacteria, *Cyanobium* spp. and *Pseudanabaena rosea* were dominant by the end of SIII, when the maximum microalgae concentration ($0.19 \cdot 10^9$ cells/L by day 217) was achieved (Richmond, 2004). The unexpected occurrence of microalgae in PBR-PPB was more likely due to the long-term duration of the experiment than to the decrease in HRT.

C. vulgaris, the microalga species inoculated in PBR-AB, was detected in all stages from day 7 to day 224, along with other *Chlorella* species. The high tolerance of microalgae from the genus *Chlorella*, which ranked 5th in the ranking of pollution tolerant microalgae species established by Palmer (1969), supported the dominance of this microalgal species in PBR-AB regardless of the HRT. In addition, the monitoring of the microalgae population structure clearly showed that the decrease in HRT induced a gradual wash-out of microalgae, which mediated a significant decrease in the number of cells from 1.8 cells/L$\cdot 10^9$ (day 84) to 0.17 cells/L$\cdot 10^9$ (day 244) under steady state in PBR-AB. This study also revealed that inoculation of the PBR-AB with a specific photosynthetic microorganism does not guarantee its long-term dominance during PWW treatment (Serejo et al., 2015). Interestingly, the stepwise decrease in HRT in

PBR-PPB occurred concomitantly with the appearance of microalgae from day 98 onwards. Finally, it should be stressed that no direct correlation between the structure of microalgae population in the PBRs and the structure of bacterial population was found (Fig. 4, 5).

< Fig. 5>

3.2.5 Bacteria population structure

The bacterial analysis of the microbial communities present in PBR-AB revealed the occurrence of the following phyla at varying abundances along the three operational stages: *Actinobacteria, Chloroflexi, Cyanobacteria, Epsilonbacteraeota, Firmicutes, Patescibacteria and Proteobacteria* among others phyla. *Proteobacteria and Cyanobacteria* represented the main phyla present in the inoculum of PBR-AB, with shares of 67.1 and 26.9, respectively. All phyla were detected in SI and SII in PBR-AB under steady state, although the phylum *Actinobacteria* was not present in SIII. The decrease in HRT induced a severe swift in the structure of the bacterial community, represented by *Firmicutes* (43.8%), *Epsilonbacteraeota* (10.7%), *Chloroflexi* (9.3%) *Proteobacteria* (10.9%) and *Cyanobacteria* (13.2%) at the end of the experiment (Table 2). On the other hand, the bacterial analysis in PBR-PPB revealed the occurrence of the phyla *Acidobacteria, Chloroflexi, Epsilonbacteraeota, Firmicutes, Patescibacteria, Proteobacteria and Synergistetes* among others. *Proteobacteria* and *Synergistetes* accounted for 83.8 and 5.3% of the bacteria in the inoculum of PBR-PPB. *Epsilonbacteraeota, Firmicutes and Proteobacteria* were dominant along the three stages, while *Patescibacteria, w*hich was present in SI and SII, was not detected in SIII. The decrease in HRT in PBR-PPB mediated the dominance of *Firmicutes* and *Epsilonbacteraeota* (46.7 % and 19.8 % of abundance) and decreased the contribution

of *Proteobacteria* to 19.8% in SIII (Table 2). Overall, the HRT seems to play a key role on the bacterial population structure in both PBR-AB and PBR-PPB during PWW treatment. *Firmicutes* is one of two dominant phyla in the large intestine of human and pig (Ban-Tokuda et al., 2017). *Firmicutes* can degrade volatile fatty acids, which typically account for 80% of the TOC in the soluble fraction of PWW (Ferrero et al., 2012).

< Table 2 >

Only the *Proteobacteria* phylum, which comprise the purple photosynthetic bacteria group, was monitored in this study in PBR-PPB. *Proteobacteria* was the main phylum with 67.1 and 83.8 % of the species present in the inocula of PBR-AB and PBR-PPB, respectively (Fig. 6). Interestingly, *Alphaproteobacteria* was the only class found in both photobioreactors within the *Proteobacteria* phylum. *Blastomonas*, which are aerobic and catalase/oxidase-positive, was the dominant genus in the inoculum of PBR-AB with 49.7% of the total number of bacteria (Castro et al., 2017). However, *Blastomonas* was not found in PBR-AB during SI, SII and SIII. *Rhodoplanes* was detected in PBR-AB during SII (18.7% of the total number of bacteria) and SIII (1.5%), while *Rhodobacter* was only present in SIII (6.5%), despite both genera belong to PPB (Hunter et al., 2009)(Hiraishi and Ueda, 1994)(Fig. 6a). On the other hand, *Rhodopseudomonas* was the dominant genus in the inoculum of PBR-PPB with 81.7% of the total number of bacteria, but disappeared from SII onwards (Fig. 6b). *Rhodopseudomonas* are purple non-sulfur phototropic bacteria (Hiraishi and Ueda, 1994) that can metabolize organic substrates (Cheah et al., 2016). The phototrophic *Rhodoplanes* accounted for 9.2, 11.4 and 7.5% of the total number of bacteria in SI, SII and SIII, respectively (Hunter et al., 2009) (Hiraishi and Ueda, 1994). In this context, a

wash-out of *Rhodopseudomonas* followed by the dominance of *Rhodoplanes* was also observed by Chitapornpan et al., (2013) in a membrane PPB-based photobioreactor during the treatment of food processing wastewater.

Finally, the Shannon-Wiener diversity indexes calculated in both photobioreactors indicated an increase in diversity compared to the inocula, which remained similar during process operation. Thus, the values of *H* in the inoculum, SI, SII and SIII were, respectively, 0.74, 1.89, 1.64 and 1.69 in PBR-AB, and 0.53, 1.32, 1.68 and 1.48 in PBR-PPB. This low-bacterial diversity in both photobioreactors was likely due to the high toxicity of the PWW treated and the low HRT used in this study.

< Fig. 6>

4. Conclusions

This work constitutes, to the best of our knowledge, the first comparative evaluation of the potential of microalgae and PPB during continuous PWW treatment in open photobioreactors. This research revealed a similar treatment performance of both photosynthetic microorganisms in terms of carbon, nutrients and zinc removal. The PBR-PPB exhibited a slightly better capacity to remove organic matter, which was not observed during batch PWW treatment. Interestingly, a superior carbon and nutrient recovery was recorded in PBR-AB. The stepwise decrease in HRT, rather than the type of illumination used, caused significant changes in the structure of microalgae and bacterial population.

5. Acknowledgments

This research was supported by the Spanish Ministry of Science, Innovation and Universities, the FEDER EU program (CTQ2017-84006-C3-1-R), and the Regional Government of Castilla y León (UIC 71). The financial support from the program EURICA (Erasmus Mundus Action 2, Strand 1, Lot 15, Grant Agreement number 2013-2587) and Universidad Nacional Autónoma de Nicaragua (UNAN-Managua) is also gratefully acknowledged.

References

1. APHA, 2005. Standards Methods for the Examination of Water and Wastewater, 21 st. ed. American Public Health Association, American Water Works Association, Water Enviroment Federation, Washington,D.C.

2. Ban-Tokuda, T., Maekawa, S., Miwa, T., Ohkawara, S., Matsui, H., 2017. Changes in faecal bacteria during fattening in finishing swine. Anaerobe 47, 188–193. doi:10.1016/j.anaerobe.2017.06.006

3. Bastos, R.G., Queiroz, Zepka, L.Q., Volpato, G., García, Jacob-Lopes, 2009. COD Removal of Parboilized Rice Wastewater By Cyanobacteria Aphanothece Microscopica Nägeli. BioEng, Campinas 3, 245–250.

4. Bertling, K., Hurse, T.J., Kappler, U., Rakic, A.D., Sciences, M., 2006. Lasers — An Effective Artificial Source of Radiation for the Cultivation of Anoxygenic Photosynthetic Bacteria. Biotechnology and Bioengineering 94, 337–345. doi:10.1002/bit

5. Cabanelas, I.T.D., Ruiz, J., Arbib, Z., Chinalia, F.A., Garrido-Pérez, C., Rogalla, F., Nascimento, I.A., Perales, J.A., 2013. Comparing the use of different domestic wastewaters for coupling microalgal production and nutrient removal. Bioresource

Technology 131, 429–436. doi:10.1016/j.biortech.2012.12.152

6. Castro, D.J., Llamas, I., Béjar, V., Martínez-Checa, F., 2017. Blastomonas quesadae sp. Nov., isolated from a saline soil by dilution-to-extinction cultivation. International Journal of Systematic and Evolutionary Microbiology 67, 2001–2007. doi:10.1099/ijsem.0.001902

7. Cheah, W.Y., Ling, T.C., Show, P.L., Juan, J.C., Chang, J.S., Lee, D.J., 2016. Cultivation in wastewaters for energy: A microalgae platform. Applied Energy 179, 609–625. doi:10.1016/j.apenergy.2016.07.015

8. Chitapornpan, S., Chiemchaisri, C., Chiemchaisri, W., Honda, R., Yamamoto, K., 2013. Organic carbon recovery and photosynthetic bacteria population in an anaerobic membrane photo-bioreactor treating food processing wastewater. Bioresource Technology 141, 65–74. doi:10.1016/j.biortech.2013.02.048

9. Craggs, R., Sutherland, D., Campbell, H., 2012. Hectare-scale demonstration of high rate algal ponds for enhanced wastewater treatment and biofuel production. Journal of Applied Phycology 24, 329–337. doi:10.1007/s10811-012-9810-8

10. Dassey, A.J., Theegala, C.S., 2013. Harvesting economics and strategies using centrifugation for cost effective separation of microalgae cells for biodiesel applications. Bioresource Technology 128, 241–245. doi:10.1016/j.biortech.2012.10.061

11. de Godos, I., Arbib, Z., Lara, E., Rogalla, F., 2016. Evaluation of High Rate Algae Ponds for treatment of anaerobically digested wastewater: Effect of CO2addition and modification of dilution rate. Bioresource Technology 220, 253–261. doi:10.1016/j.biortech.2016.08.056

12. de Godos, I., Vargas, V.A., Blanco, S., González, M.C.G., Soto, R., García-Encina, P.A., Becares, E., Muñoz, R., 2010. A comparative evaluation of microalgae for

the degradation of piggery wastewater under photosynthetic oxygenation. Bioresource Technology 101, 5150–5158. doi:10.1016/j.biortech.2010.02.010

13. de Lima, L.K.F., Ponsano, E.H.G., Pinto, M.F., 2011. Cultivation of Rubrivivax gelatinosus in fish industry effluent for depollution and biomass production. World Journal of Microbiology and Biotechnology 27, 2553–2558. doi:10.1007/s11274-011-0725-3

14. Engelbrektson, A., Kunin, V., Wrighton, K.C., Zvenigorodsky, N., Chen, F., Ochman, H., Hugenholtz, P., 2010. Experimental factors affecting PCR-based estimates of microbial species richness and evenness. The ISME Journal 4, 642–647. doi:10.1038/ismej.2009.153

15. Ferrero, E.M., de Godos, I., Rodríguez, E.M., García-Encina, P.A., Muñoz, R., Bécares, E., 2012. Molecular characterization of bacterial communities in algal-bacterial photobioreactors treating piggery wastewaters. Ecological Engineering 40, 121–130. doi:10.1016/j.ecoleng.2011.10.001

16. Franchino, M., Tigini, V., Varese, G.C., Mussat Sartor, R., Bona, F., 2016. Microalgae treatment removes nutrients and reduces ecotoxicity of diluted piggery digestate. Science of The Total Environment 569, 40–45. doi:10.1016/j.scitotenv.2016.06.100

17. García, D., Alcántara, C., Blanco, S., Pérez, R., Bolado, S., Muñoz, R., 2017a. Enhanced carbon, nitrogen and phosphorus removal from domestic wastewater in a novel anoxic-aerobic photobioreactor coupled with biogas upgrading. Chemical Engineering Journal 313, 424–434. doi:10.1016/j.cej.2016.12.054

18. García, D., Posadas, E., Blanco, S., Acién, G., García-Encina, P., Bolado, S., Muñoz, R., 2018. Evaluation of the dynamics of microalgae population structure and process performance during piggery wastewater treatment in algal-bacterial

photobioreactors. Bioresource Technology 248, 120–126. doi:10.1016/j.biortech.2017.06.079

19. García, D., Posadas, E., Grajeda, C., Blanco, S., Martínez-Páramo, S., Acién, G., García-Encina, P., Bolado, S., Muñoz, R., 2017b. Comparative evaluation of piggery wastewater treatment in algal-bacterial photobioreactors under indoor and outdoor conditions. Bioresource Technology 245, 483–490. doi:10.1016/j.biortech.2017.08.135

20. Golomysova, A., Gomelsky, M., Ivanov, P.S., 2010. Flux balance analysis of photoheterotrophic growth of purple nonsulfur bacteria relevant to biohydrogen production. International Journal of Hydrogen Energy 35, 12751–12760. doi:10.1016/j.ijhydene.2010.08.133

21. González-Fernández, C., García-Encina, P.A., 2009. Impact of substrate to inoculum ratio in anaerobic digestion of swine slurry. Biomass and Bioenergy 33, 1065–1069. doi:10.1016/j.biombioe.2009.03.008

22. González, E., Díaz, O., Ruigómez, I., de Vera, C.R., Rodríguez-Gómez, L.E., Rodríguez-Sevilla, J., Vera, L., 2017. Photosynthetic bacteria-based membrane bioreactor as post-treatment of an anaerobic membrane bioreactor effluent. Bioresource Technology 239, 528–532. doi:10.1016/j.biortech.2017.05.042

23. Hernández, D., Riaño, B., Coca, M., García-González, M.C., 2013. Treatment of agro-industrial wastewater using microalgae-bacteria consortium combined with anaerobic digestion of the produced biomass. Bioresource Technology 135, 598–603. doi:10.1016/j.biortech.2012.09.029

24. Hiraishi, A., Ueda, Y., 1994. Rhodoplanes gen. nov., a New Genus of Phototrophic Bacteria Including Rhodopseudomonas rosea as Rhodoplanes roseus comb. nov. and Rhodoplanes elegans sp. nov. International Journal of Systematic Bacteriology 44, 665–673. doi:10.1099/00207713-44-4-665

25. Hülsen, T., Barry, E.M., Lu, Y., Puyol, D., Batstone, D.J., 2016a. Low temperature treatment of domestic wastewater by purple phototrophic bacteria: Performance, activity, and community. Water Research 100, 537–545. doi:10.1016/j.watres.2016.05.054

26. Hülsen, T., Barry, E.M., Lu, Y., Puyol, D., Keller, J., Batstone, D.J., 2016b. Domestic wastewater treatment with purple phototrophic bacteria using a novel continuous photo anaerobic membrane bioreactor. Water Research 100, 486–495. doi:10.1016/j.watres.2016.04.061

27. Hülsen, T., Batstone, D.J., Keller, J., 2014. Phototrophic bacteria for nutrient recovery from domestic wastewater. Water Research 50, 18–26. doi:10.1016/j.watres.2013.10.051

28. Hülsen, T., Hsieh, K., Lu, Y., Tait, S., Batstone, D.J., 2018. Simultaneous treatment and single cell protein production from agri-industrial wastewaters using purple phototrophic bacteria or microalgae – A comparison. Bioresource Technology 254, 214–223. doi:10.1016/j.biortech.2018.01.032

29. Hunter, C.N., Daldal, F., Thurnauer, M.C., Beatty, J.T., 2009. The Purple Phototrophic Bacteria. doi:10.1007/978-1-4020-8815-5

30. Javanbakht, V., Alavi, S.A., Zilouei, H., 2014. Mechanisms of heavy metal removal using microorganisms as biosorbent. Water Science and Technology 69, 1775–1787. doi:10.2166/wst.2013.718

31. Kantachote, D., Torpee, S., Umsakul, K., 2005. The potential use of anoxygenic phototrophic bacteria for treating latex rubber sheet wastewater. Electronic Journal of Biotechnology 8, 314–323. doi:10.2225/vol8-issue3-fulltext-8

32. Kaplan, D., Cristiaen, D., Shoshana, A., 1987. Chelating Properties of Extracellular Polysaccharides from Chlorella spp. Applied and Environmental

Microbiology. 53, 2953–2956.

33. Madukasi, E.I., Dai, X., He, C., Zhou, J., 2010. Potentials of phototrophic bacteria in treating pharmaceutical wastewater. Int. J Environ. Sci. Tech 7, 165–174.

34. Mateo-sagasta, J., Burke, J., 2012. Agriculture and water quality interactions: a global overview. SOLAW Background Thematic Report - TR08.

35. Myung, K.K., Choi, K.M., Yin, C.R., Lee, K.Y., Im, W.T., Ju, H.L., Lee, S.T., 2004. Odorous swine wastewater treatment by purple non-sulfur bacteria, Rhodopseudomonas palustris, isolated from eutrophicated ponds. Biotechnology Letters 26, 819–822. doi:10.1023/B:BILE.0000025884.50198.67

36. Oswald, W.J., Gotaas, H.B., Golueke, C.G., Kellen, W.R., Gloyna, E.F., Hermann, E.R., 1957. Algae in Waste Treatment [with Discussion]. Water Environment Federation 29, 437–457. doi:10.2307/25033322

37. Palmer, C.M., 1969. A composite rating of algae tolerating organic pollution. J. Phicol 5, 78–82.

38. Posadas, E., Marín, D., Blanco, S., Lebrero, R., Muñoz, R., 2017. Simultaneous biogas upgrading and centrate treatment in an outdoors pilot scale high rate algal pond. Bioresource Technology 232, 133–141. doi:10.1016/j.biortech.2017.01.071

39. Richmond, A., 2004. Handbook of microalgal culture: biotechnology and applied phycology/edited by Amos Richmond. doi:10.1002/9780470995280

40. Rittmann, B.E., McCarty, P.L., 2012. Environmental Biotechnology:Principles and Applications, 1 st. ed. Tata McGraw-Hill, New Delhi.

41. Serejo, M.L., Posadas, E., Boncz, M.A., Blanco, S., García-Encina, P., Muñoz, R., 2015. Influence of biogas flow rate on biomass composition during the optimization of biogas upgrading in microalgal-bacterial processes. Environmental Science and Technology 49, 3228–3236. doi:10.1021/es5056116

42. Sournia, A., 1978. Phytoplankton manual. UNESCO, Paris.

43. statista, 2018. Global pork production in 2017, by country [WWW Document]. URL https://www.statista.com (accessed 5.10.18).

44. Tigini, V., Franchino, M., Bona, F., Varese, G.C., 2016. Is digestate safe? A study on its ecotoxicity and environmental risk on a pig manure. The Science of the total environment 551–552, 127–132. doi:10.1016/j.scitotenv.2016.02.004

45. Zhang, D., Yang, H., Zhang, W., Huang, Z., 2003. Rhodocista pekingensis sp . nov ., a cyst-forming phototrophic bacterium from a municipal wastewater treatment plant. International Journal of Systematic and Evolutionary Microbiology 53, 1111–1114. doi:10.1099/ijs.0.02500-0

Figure captions

Fig. 1. Schematic diagram of the algal-bacterial photobioreactor (PBR-AB) and purple photosynthetic bacteria photobioreactor (PBR-PPB) treating diluted PWW. IR-LED: Infrared Light Emitting Diodes; PAR-LED: Photosynthetic Active Radiation Light Emitting Diodes.

Fig. 2. Time course of the concentration of TOC (a), TN (b) and TSS (c) in the algal-bacterial and purple photosynthetic bacteria systems during the batch biodegradation of piggery wastewater diluted at 5%, 10% and 15%.

Fig. 3. Steady state removal efficiencies of TOC (a), IC (b), TN (c), NH_4^+ (d) and TP (e) in PBR-AB and PBR-PPB in the three operational stages evaluated. Upper bold numbers indicate the steady state removal efficiencies, while vertical bars represent the standard deviation from replicate measurements during steady state operation. Stage I, II and III correspond to HRTs of 10.6, 7.6 and 4.1 days, respectively.

Fig. 4. Time course of TSS concentration in, PBR-AB, PBR-PPB and PWW during the entire experiment.

Fig. 5. Time course of the microalgae population structure in PBR-AB (a) and PBR-PPB (b) during the three operational stages.

Fig. 6. Relative abundance (%) of genera belonging to the phylum *Proteobacteria* in the inocula and cultivation broth of PBR-AB (**a**) and PBR-PPB (**b**) along the three operational stages. The abundance was calculated based on the total number of bacteria.

Figure
Click here to download Figure: Figure1.docx

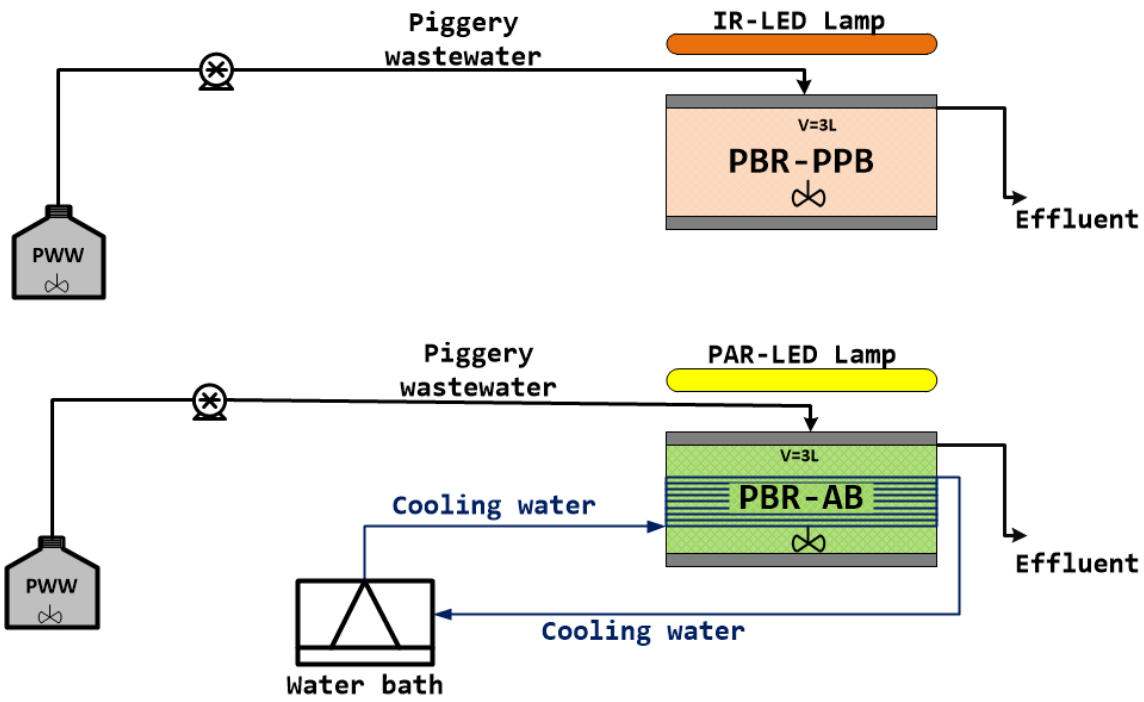

Fig. 1. Schematic diagram of the algal-bacterial photobioreactor (PBR-AB) and purple photosynthetic bacteria photobioreactor (PBR-PPB) treating diluted PWW. IR-LED: Infrared Light Emitting Diodes; PAR-LED: Photosynthetic Active Radiation Light Emitting Diodes.

Figure
Click here to download Figure: Figure2.docx

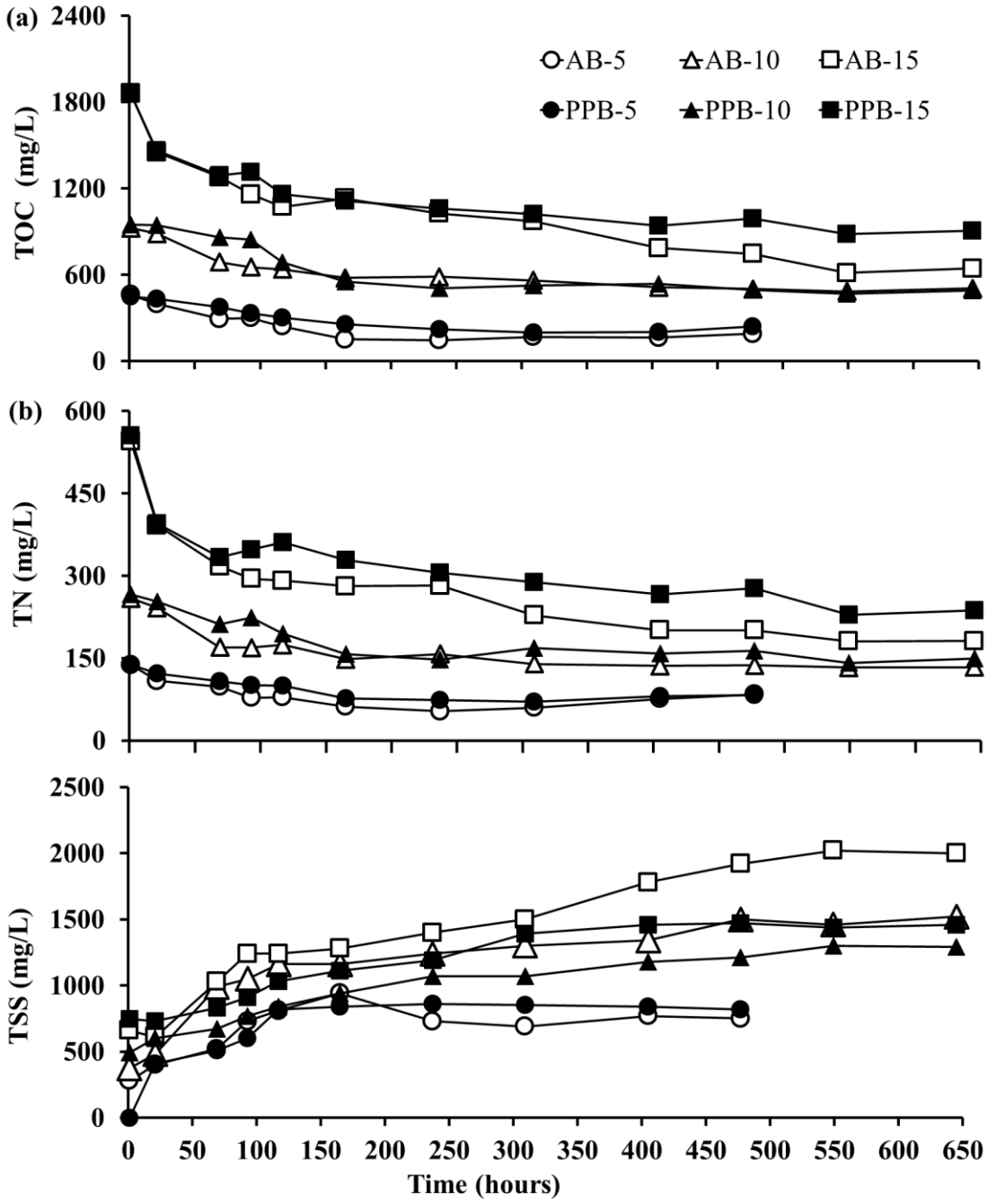

Fig. 2. Time course of the concentration of TOC (**a**), TN (**b**) and TSS (**c**) in the algal-bacterial and purple photosynthetic bacteria systems during the batch biodegradation of piggery wastewater diluted at 5%, 10% and 15%.

Figure
Click here to download Figure: Figure3.docx

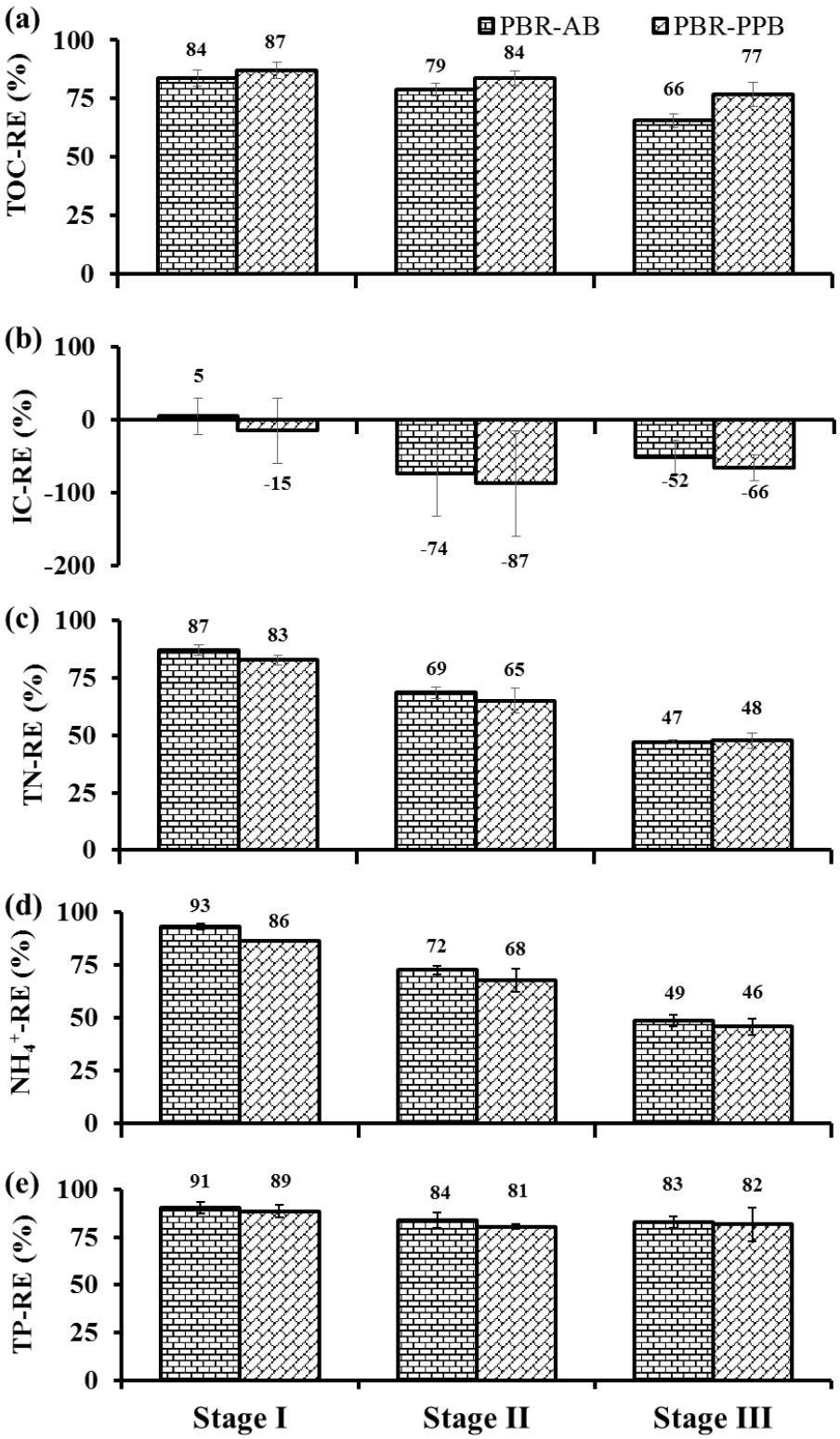

Fig. 3. Steady state removal efficiencies of TOC (**a**), IC (**b**), TN (**c**), NH_4^+ (**d**) and TP (**e**) in PBR-AB and PBR-PPB in the three operational stages evaluated. Upper bold numbers indicate the steady state removal efficiencies, while vertical bars represent the

standard deviation from replicate measurements during steady state operation. Stage I, II and III correspond to HRTs of 10.6, 7.6 and 4.1 days, respectively.

Figure
Click here to download Figure: Figure4.docx

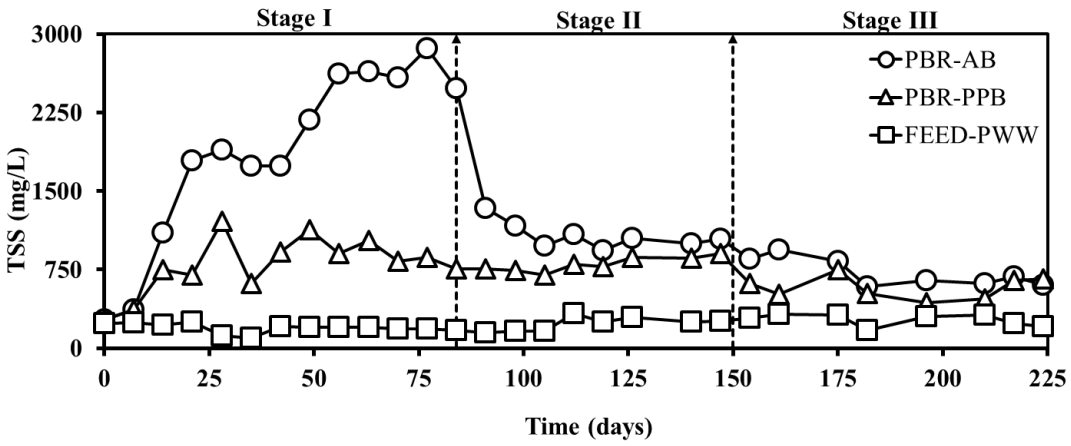

Fig. 4. Time course of TSS concentration in, PBR-AB, PBR-PPB and PWW during the entire experiment.

Figure

Click here to download Figure: Figure5.docx

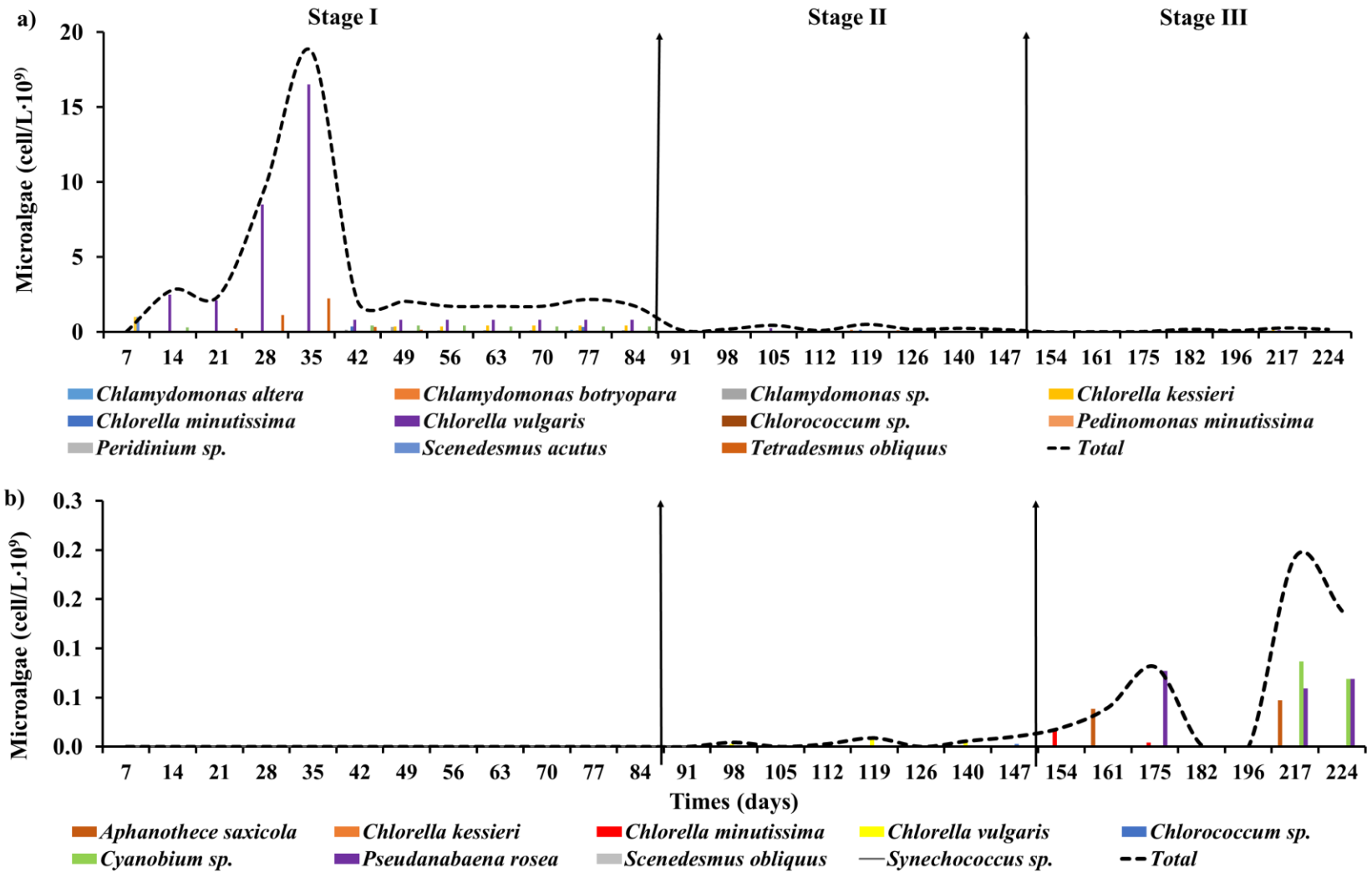

Fig. 5. Time course of the microalgae population structure in PBR-AB (**a**) and PBR-PPB (**b**) during the three operational stages.

Figure
Click here to download Figure: Figure6.docx

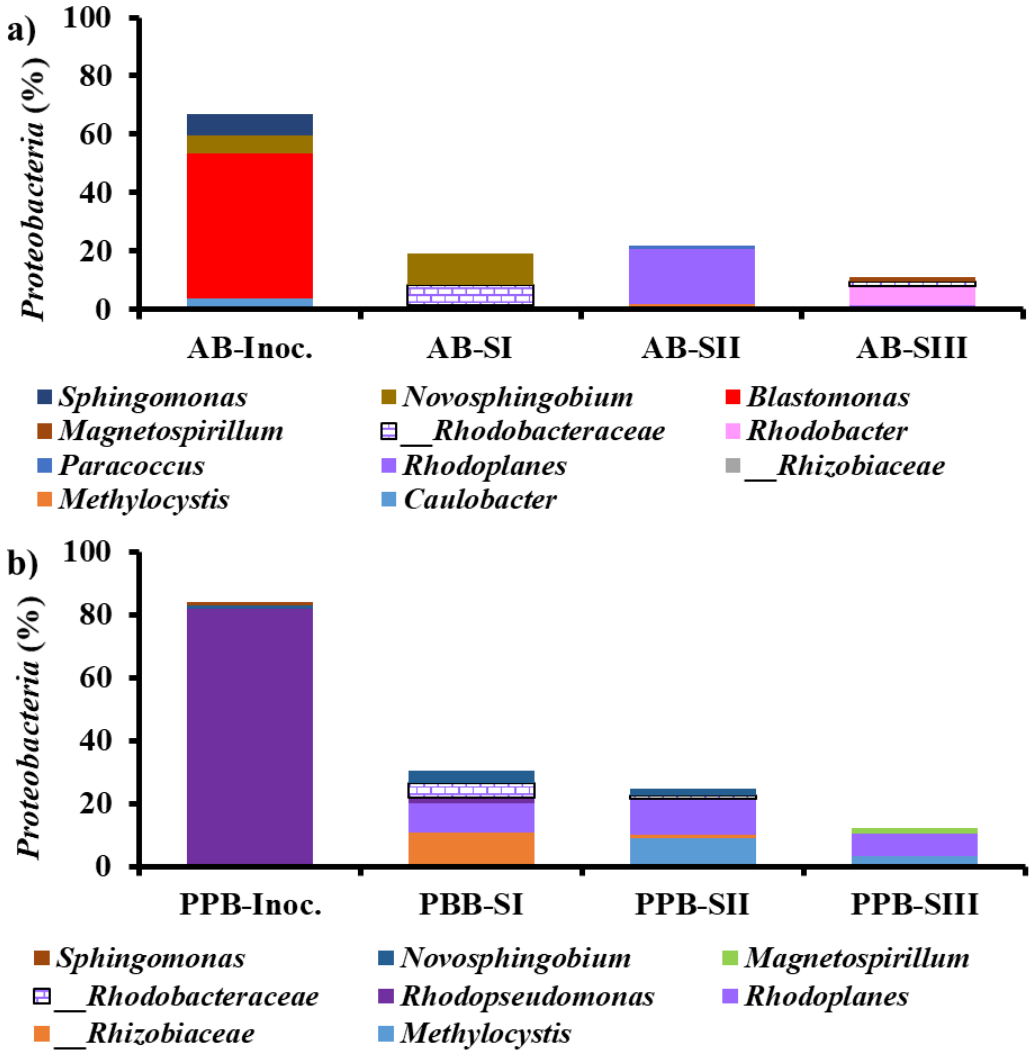

Fig. 6. Relative abundance (%) of genera belonging to the phylum *Proteobacteria* in the inocula and cultivation broth of PBR-AB (**a**) and PBR-PPB (**b**) along the three operational stages. The abundance was calculated based on the total number of bacteria.

Table

Table 1. Operational conditions and physical/chemical characterization of the diluted PWW and cultivation broth in PBR-AB and PBR-PPB during steady state along the three operational stages under continuous operation.

Parameters		PWW	Stage I		Stage II		Stage III	
			PBR-AB	PBR-PPB	PBR-AB	PBR-PPB	PBR-AB	PBR-PPB
Operational days		-	84		63		77	
HRT (days)		-	≈ 10.6		≈ 7.6		≈ 4.1	
pH (units)		-	8.7±0.1	8.6±0.1	8.7±0.1	8.7±0.1	8.5±0.1	8.5±0.3
Light intensity of PAR (µmol/m^2·s)		-	1388±39	-	1379±33	-	1407±12	-
Light intensity of IR (W/m^2)		-	-	50±6	-	46±1	-	48±8
Temperature (◦C)	09h00	-	32.8±0.9	30.4±1.4	31.3±1.0	28.4±1.5	32.1±0.9	30.5±1.4
	16h00	-	31.2±1.5	30.5±1.5	30.3±1.5	29.0±1.5	30.7±1.6	30.3±1.5
Dissolved oxygen (mg/L)		-	0.04±0.02	0.05±0.02	0.03±0.02	0.02±0.01	0.03±0.02	0.03±0.02
Evaporation rates (%)		-	72±7	56±8	42±5	36±5	21±2	18±3
***TOC (mg/L)**		574±16	309±18	181±54	199±9	136±3	246±31	156±31
***IC (mg/L)**		58±4	169±17	142±3	144±10	137±7	117±13	122±15
***TN (mg/L)**		166±9	68±5	65±4	85±3	84±6	118±9	110±10
***Ammonium (mg/L)**		179±5	41±3	60±7	80±5	83±6	118±14	118±6
***Nitrate (mg/L)**		< 0.5	< 0.5	< 0.5	< 0.5	< 0.5	< 0.5	< 0.5
***Nitrite (mg/L)**		< 0.5	< 0.5	< 0.5	< 0.5	< 0.5	< 0.5	< 0.5
***TP (mg/L)**		5.65±0.41	1.62±0.61	1.35±0.51	1.62±0.43	1.75±0.27	1.22±0.27	1.22±0.57
***Zinc (mg/L)**		0.78±0.07	0.07±0.03	0.15±0.02	0.08±0.02	0.12±0.02	0.08±0.02	0.06±0.01
***TSS (mg/L)**		237±63	2640±161	873±114	1005±54	853±51	638±35	553±118
- Not applicable								
* Average values and standard deviation obtained under steady stage conditions								

Table 2. Taxonomic report of the bacteria present in PBR-AB and PBR-PPB.

Phyllum	**PBR-AB (%)**				**PBR-PPB (%)**			
	Inoc.	**SI**	**SII**	**SIII**	**Inoc.**	**SI**	**SII**	**SIII**
Acidobacteria						0.5	2.5	1.5
Actinobacteria		1.3	3.4					
Chloroflexi		13.2	11.3	9.3			3.7	5.4
Cyanobacteria	26.9	25.7	3.1	13.2				
Epsilonbacteraeota		18.8	8.2	10.7		46.6	19.9	19.8
Firmicutes	1.0	4.7	38.2	43.8	3.6	5.3	29.3	46.7
Patescibacteria		5.5	0.6	1.0	0.0	4.5	6.5	
Proteobacteria	67.1	19.1	21.6	10.9	83.8	30.5	24.6	12.1
Synergistetes					5.3			
Other	5.0	11.8	13.5	11.1	7.3	12.6	13.5	14.4
Total nº of Cells	34903	18964	13683	28884	44503	29644	19355	14765

Electronic Annex

Click here to download Electronic Annex: Supplementary Materials.docx